processes

MDPI

Article

A Novel Approach for Voltage Stability Assessment and Optimal Siting and Sizing of DGs in Radial Power Distribution Networks

Salah Mokred [1], Yifei Wang [1,*], Mohammed Alruwaili [2] and Moustafa Ahmed Ibrahim [3,*]

[1] Electrical Engineering Department, Southeast University, Nanjing 210096, China; salah_mokred@seu.edu.cn
[2] Department of Electrical Engineering, College of Engineering, Northern Border University, Arar 91431, Saudi Arabia; mohammed.alruwailir@nbu.edu.sa
[3] Electrical Engineering Department, University of Business and Technology, Jeddah 23435, Saudi Arabia
* Correspondence: wyf@seu.edu.cn (Y.W.); m.ibrahim@ubt.edu.sa (M.A.I.)

Abstract

The increasing integration of renewable energy sources and the rising demand for electricity has intensified concerns over voltage stability in radial distribution systems. These networks are particularly susceptible to voltage collapse under heavy loading conditions, posing serious system reliability and efficiency risks. Integrating distributed generation (DG) has emerged as a strategic solution to strengthen voltage profiles and reduce power losses. To address this challenge, this study proposes a novel distribution voltage stability index (*NDVSI*) for accurately assessing voltage stability and guiding optimal DG placement and sizing. The *NDVSI* provides a reliable tool to identify weak buses and their neighboring nodes that critically impact stability. By targeting these locations, the method ensures DG units are installed where they offer maximum improvement in voltage support and minimum power losses. The approach is implemented using MATLAB R2019a (MathWorks Inc., Natick, MA, USA) and validated on three benchmark radial distribution systems, including IEEE 12-bus, 33-bus, and 69-bus systems, demonstrating its scalability and effectiveness across different grid complexities. Comparative analysis with existing voltage stability indices confirms the superiority of *NDVSI* in both diagnostic precision and practical application. The proposed approach offers a technically sound and economically viable tool for enhancing the reliability, stability, and performance of modern distribution networks.

Keywords: *NDVSI*; voltage stability assessment; distributed generation (DG); radial distribution systems

check for updates

Academic Editor: Michael C. Georgiadis

Received: 22 May 2025
Revised: 16 June 2025
Accepted: 20 June 2025
Published: 14 July 2025

Citation: Mokred, S.; Wang, Y.; Alruwaili, M.; Ibrahim, M.A. A Novel Approach for Voltage Stability Assessment and Optimal Siting and Sizing of DGs in Radial Power Distribution Networks. *Processes* **2025**, *13*, 2239. https://doi.org/10.3390/pr13072239

Copyright: © 2025 by the authors. Licensee MDPI, Basel, Switzerland. This article is an open access article distributed under the terms and conditions of the Creative Commons Attribution (CC BY) license (https://creativecommons.org/licenses/by/4.0/).

1. Introduction

The electric power system comprises the interconnected elements of generation, transmission, distribution, and consumption. Distribution networks are commonly configured in a radial manner, with a single, unified direction of power flow. Contemporary distribution power systems encounter various challenges as a result of the continuous increase in energy demand. The application of various distributed power sources, such as distributed generation (DG) systems, flexible AC transmission systems (FACTS), and other technologies, has led to the development of several placement strategies for DGs, as suggested in the literature [1]. Overloading in power systems can trigger voltage collapse, making accurate detection of critical limits vital for system stability [2]. These advancements aim to tackle the growing challenges and demands of modern power systems. Around 30% of energy

losses occur during the transmission phase, while approximately 70% happen during the distribution phase [3]. Although the target was to limit distribution losses to 7.5% of the total generation, actual losses have reached a significantly higher level of 15.5% [4]. As a result, the focus has shifted toward improving the effectiveness and performance of distribution systems, as this phase plays a significant role in overall energy losses. Addressing these issues is essential for enhancing system stability and reliability, as well as minimizing energy losses.

Current research focuses on using various technologies to improve stability margin and lower energy losses in distribution networks. These initiatives are essential to raising the efficiency, stability, and dependability of the electricity distribution system. As renewable energy sources become more widely integrated, distributed generators (DGs) are essential for enhancing power systems' stability and reliability. DGs play a significant role in preventing voltage collapse, particularly during peak load periods when traditional power supplies may struggle to maintain stability. Additionally, they contribute to reducing energy losses by producing power nearer to the demand point, thus decreasing the necessity for long-distance transmission. In addition, the integration of DGs strengthens the system's stability margin by providing localized support, enhancing voltage regulation, and creating a more reliable and stable power supply throughout the distribution network. Distribution generators also have a significant impact on both the economic and environmental aspects of power systems. By reducing the reliance on fossil fuels, which are major contributors to carbon emissions, DGs help mitigate environmental pollution.

Additionally, they lower the cost of fuel consumption and reduce energy losses, leading to overall savings in operational costs. This dual benefit promotes a cleaner energy future and enhances the financial sustainability of power systems, making DGs a crucial element in modern energy strategies. The study in [5] highlights that the generation capacity of distribution generators ranges from 5 to 50 MW. Recently, DGs powered by renewable energy sources (RESs) have experienced rapid global growth, driven by the need to reduce CO_2 emissions, power losses, and fuel consumption [6–8]. This trend reflects a growing shift toward cleaner and more efficient energy solutions, contributing to environmental sustainability and improved energy efficiency. Studies [9,10] focus on maximizing the economic benefits for owners by integrating DG units into the optimal locations within transmission and distribution systems. Recent work highlights that vehicle-to-grid integrated virtual power plants can support voltage stability by mitigating voltage drops and reducing network stress under high electric vehicle penetration [11]. Placing DG units in the optimal locations and selecting the appropriate size improves the system's technical operation and cost-effectiveness. This is demonstrated in Figure 1, which illustrates the positive impact of strategic DG integration on system performance and cost-effectiveness.

The literature on DG siting and sizing employs various techniques, which can be broadly categorized into two key groups. The first group relies on optimization strategies. For instance, Werkie et al. [12] utilize an improved particle swarm optimization approach (IPSO) to mitigate power loss and enhance the voltage profile. Study [13] utilizes the bacterial foraging optimization algorithm (BFOA), whereas [14] applies the dragonfly algorithm (DFA) to identify the proper size and positioning of distributed generators. The objective function was formulated to minimize energy losses and strengthen the system's voltage stability. In [15], a backtracking search optimization algorithm (BSOA) is used to optimize the positioning of distributed generators (DGs) in radial distribution grids.

The ant lion optimization technique was presented in Reference [16] to identify the best location and capacity for DG units based on renewable energy across different distribution grids. The optimal DG location in microgrids is suggested by [17] using an advanced optimization-based approach. Radial distribution grids have been analyzed for optimal

DG placement and capacity using methods such as the hybrid PSO [18] and the stud krill herd algorithm (SKHA) [19]. The primary objective of these studies is to minimize energy losses, considering several constraints such as active power generation limit, voltage limit, and energy balance constraints. A wide range of optimization techniques has been explored in the literature for determining the best placement and sizing of various DG units, including the multi-objective whale optimization algorithm (MOWOA) [20], crow search algorithm (CSA) [21], lightning search algorithm [22], and opposition-based tuned-chaotic differential evolution (OTCDE) [23], reflecting the continued interest in refining DG integration strategies.

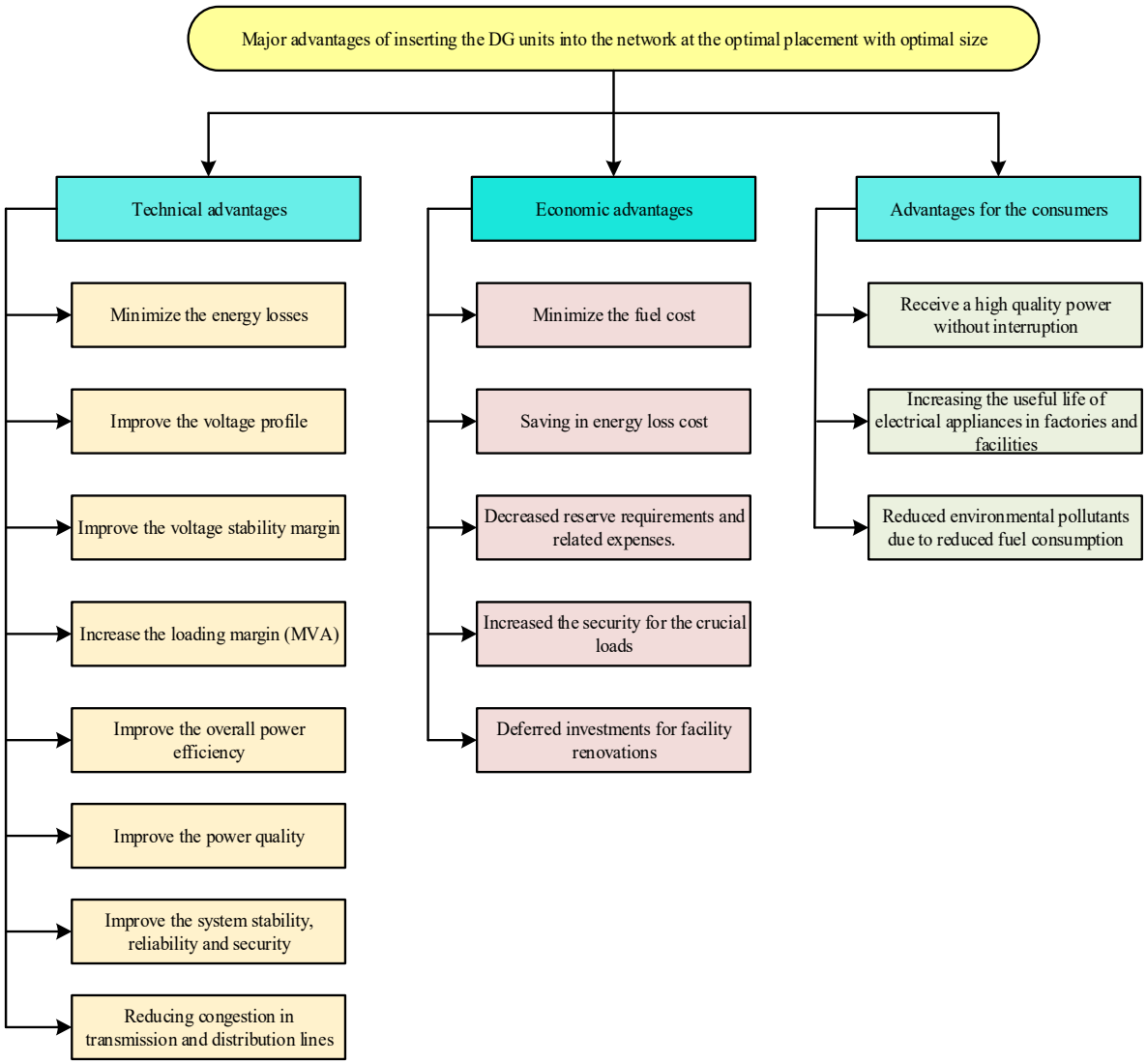


Figure 1. Classification of advantages of optimally integrating DGs into distribution systems.

The second category includes analytical approaches, which offer direct and often less computationally intensive methods compared to optimization techniques. For instance, Acharya et al. [24] utilized an exact loss formula to derive analytical expressions that aid in determining optimal DG placement and sizing. Their method provides a structured and straightforward approach. Building on this direction, Huang et al. [25] proposed an improved analytical framework capable of handling the integration of four different types of distributed generation sources. This method allows for accurately identifying suitable locations and corresponding capacities, making it adaptable to various system

configurations. Furthermore, Murty et al. [26] introduced a voltage stability index (VSI) aimed at identifying optimal DG positions on the IEEE 12-, 69- and 85-bus test systems. Their approach was benchmarked against other indices, such as the power stability index and power loss sensitivity, demonstrating improved effectiveness in enhancing voltage stability and reducing system losses. However, these methods often suffer from limited accuracy due to the limitations of the indices they rely on.

The study in [27] suggests a developed analytical approach based on a novel formula for power flow problems. This method is noniterative, direct, and without problems in convergence, even if the system contains a high R/X ratio. Moreover, studies [28–33] introduce several analytical methods for allocating and sizing DG problems. In times of reactive power deficit DGs in a radial distribution grid, a reactive compensation approach is recommended to deliver a compensated reactive power [34–36]. Studies [37–39] proposed stability indices to assess the stability in radial distribution systems. However, these indices ignore the voltage angle difference that affects the accuracy of collapse prediction. Aman et al. [32] proposed a power stability index (PSI) to indicate the candidate spots for DG allocation. However, this index disregards the effect of reactive power and gives inaccurate results when the line resistance is small.

To effectively assess voltage stability and determine optimal locations and sizes for distributed generation (DG) units, this study introduces a novel stability index named *NDVSI*. The selected references for comparison, as discussed in the case studies, were chosen based on their relevance to voltage stability assessment methods and DG integration approaches, particularly those utilizing stability indices and focusing on voltage profile improvement. The primary objective is to benchmark the proposed approach against methodologies with comparable technical foundations and goals. This focused comparison ensures a fair and meaningful evaluation of the proposed approach under similar distribution network conditions. The main contributions of this work are summarized as follows:

- Introduction of the novel distribution voltage stability index (*NDVSI*): This paper presents a newly developed voltage stability index, *NDVSI*, specifically created to assess the voltage stability within radial distribution networks. The index is tested on three well-known IEEE benchmark systems (12-bus, 33-bus, and 69-bus) to validate its performance and effectiveness. For validation and benchmarking purposes, the proposed *NDVSI* is compared against several well-established stability indices reported in the literature, highlighting its improved sensitivity, accuracy, and ability to identify weak buses more effectively.
- Identification of Candidate Buses for DG Integration: The proposed *NDVSI* is utilized alongside a systematic search technique to identify the most suitable buses for integrating distributed generation units into the network. This approach focuses on locating weak buses with low stability margins and their neighboring nodes, ensuring that DG units are placed where they can provide the greatest support in enhancing voltage stability and lowering power losses.
- Comparative Evaluation of the Proposed DG Siting and Sizing Method: To verify the performance of the suggested method for identifying the most efficient placement and size of distributed generation units, its outcomes are evaluated against those obtained from several previously published techniques. This comparative analysis demonstrates the proposed method's practical applicability, accuracy, and advantages in enhancing voltage stability and reducing power losses in radial distribution systems.
- The proposed method improves the distribution systems technically and economically.

The remaining article is organized as follows: Section 2 presents the methodology for voltage stability assessment and optimal placement and sizing of DGs. Section 3 introduces the case studies for stability assessment and DGs integration. The conclusion is presented

in Section 4. Future works have been added in Section 5. Finally, the abbreviations and nomenclature have been introduced at the end of the manuscript.

2. Methodology for Voltage Stability Assessment and Optimal Placement and Sizing of DGs

The proposed approach is applied to evaluate voltage stability and determine suitable locations within the network to integrate distributed generation units. The constant power (CP) load is only considered in this study because of space limitations. The distribution system has exceptional characteristics like a radial topology, a high R/X proportion, and imbalanced loads. The analysis of the radial distribution grids is more complex than the transmission grids since the framework of many distribution systems contains many laterals and sub-laterals, like a tree. The tree's roots provide the substation. Moreover, integrating DG units into the systems may change the system configuration. For these reasons, a topographical approach is implemented to identify the buses beyond all lines of the distribution system because of its exceptional framework, which aids in determining precisely the current that passes through all branches. Power flow analysis is performed utilizing the bus injection to branch current (BIBC) approach, as formulated in [40].

2.1. Comparison of Conventional and Proposed VSIs for Voltage Stability Assessment

The effectiveness of the proposed *NDVSI* is assessed by comparing it with several widely recognized voltage stability indices. Its applicability is demonstrated using three benchmark radial distribution networks: the IEEE 12-bus, 33-bus, and 69-bus systems. For validation purposes, the *NDVSI* results are evaluated against the stability indices *SI* [37], *SI* [38], and *SI* [39], as presented in Table 1.

Table 1. Formulation, assumptions, and threshold levels of voltage stability indices.

Index	Equation	Critical Value	Assumptions	Ref.
SI [37]	$SI = V_i^4 - 4(P_jX - Q_jR)^2 - 4V_i^2(P_jR + Q_jX)$	0.00	$\delta = 0$ and $Y = 0$	[37]
SI [38]	$SI = 0.5V_j^2 - P_jR - Q_jX$	0.00	$\delta = 0$ and $Y = 0$	[38]
SI [39]	$SI = 2V_i^2V_j^2 - V_j^4 - 2V_j^2(P_jR + Q_jX) - Z^2(P_j^2 + Q_j^2)$	0.00	$\delta = 0$ and $Y = 0$	[39]
Proposed index	$NDVSI = V_i^2 \sin^2(\theta - \delta + 45^\circ) - 2\sqrt{2}Z \sin(\theta + 45^\circ)(P_j + Q_j)$	0.00	$Y = 0$	This paper

These indices were selected due to their broad adoption in the literature, high citation frequency, and frequent application in voltage stability assessment and distributed generation (DG) placement studies. Although they share the same general abbreviation (*SI*), each of these indices originates from a different research, proposed by different authors, and they differ significantly in formulation, methodology, and performance characteristics.

To prevent ambiguity, each index is explicitly labeled with its corresponding reference as *SI* [37], *SI* [38], and *SI* [39]. These indices are based on different mathematical derivations from power flow equations and exhibit varying sensitivities to system operating conditions. For example, under base case loading, *SI* [38] typically yields a value near 0.5, while *SI* [37], *SI* [39], and the proposed *NDVSI* return values close to one, indicating that the system possesses a high stability margin. This observation is consistent with the fact that lower index values, approaching zero, signify proximity to voltage collapse. When the system is subjected to increased active, reactive, or apparent power loading, the indices exhibit different behaviors in identifying critical stress conditions, which are discussed in detail in the case studies section.

Furthermore, while all indices assume negligible shunt admittances in radial distribution systems, the proposed *NDVSI* introduces a key improvement by incorporating

voltage angle differences into its formulation. In contrast, the traditional indices do not account for this factor, which can impact accuracy under certain loading conditions. These distinctions highlight the need for individual treatment of each index in the comparative analysis and reinforce the unique advantages of the proposed *NDVSI*. Detailed formulations and comparative results are summarized in Table 1 and further analyzed throughout the simulation results.

2.2. Formulation of the Proposed Index (NDVSI)

An equivalent simple circuit of the radial distribution system, including the source at the end of bus-*i* and the load at the end of bus-*j*, is depicted in Figure 2.

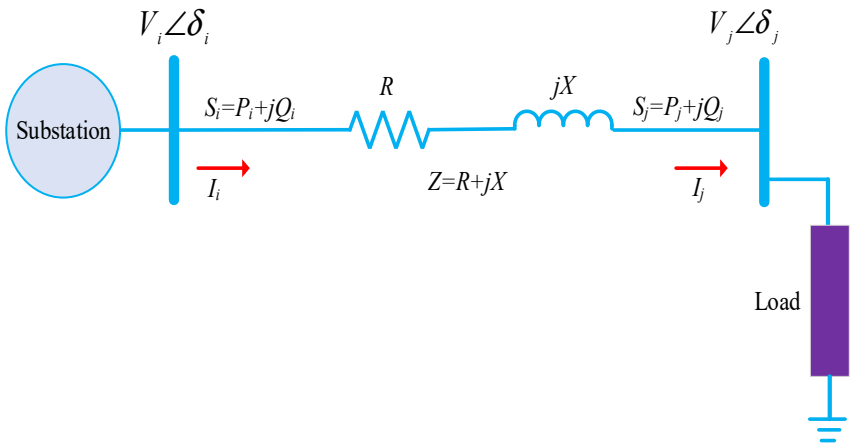


Figure 2. A simple circuit model of a radial distribution grid.

The line current can be expressed as follows:

$$I_j = \frac{|V_i|\angle\delta - |V_j|\angle 0}{Z\angle\theta} \tag{1}$$

The apparent power at the load side is expressed as follows:

$$S_j = P_j + jQ_j = V_j I_j^* \tag{2}$$

Using Equations (1) and (2), the expressions for calculating the real and reactive power delivered to the receiving terminal are derived as follows:

$$P_j = \frac{V_i V_j}{Z}\cos(\theta - \delta) - \frac{V_j^2}{Z}\cos(\theta) \tag{3}$$

$$Q_j = \frac{V_i V_j}{Z}\sin(\theta - \delta) - \frac{V_j^2}{Z}\sin(\theta) \tag{4}$$

where $\delta = \delta_i - \delta_j$ denotes the difference in voltage angles. By rearranging (3) and (4), the following expression is obtained:

$$V_j^2\cos(\theta) - V_i V_j\cos(\theta - \delta) + ZP_j = 0 \tag{5}$$

$$V_j^2\sin(\theta) - V_i V_j\sin(\theta - \delta) + ZQ_j = 0 \tag{6}$$

When both sides of Equations (5) and (6) are added together, the resulting equation is expressed as follows:

$$V_j^2(\cos(\theta) + \sin(\theta)) - V_i V_j(\cos(\theta - \delta) + \sin(\theta - \delta)) + Z(P_j + Q_j) = 0 \tag{7}$$

Equation (7) can be expressed in a simpler form as follows:

$$\sqrt{2}V_j^2 \sin(\theta + 45^\circ) - \sqrt{2}V_i V_j \sin(\theta - \delta + 45^\circ) + Z(P_j + Q_j) = 0 \quad (8)$$

Equation (8) represents the quadratic form of the voltage expression, and a real solution is achievable only when the discriminant is zero or positive, which is expressed as follows:

$$2V_i^2 \sin^2(\theta - \delta + 45^\circ) - 4\sqrt{2}Z \sin(\theta + 45^\circ)(P_j + Q_j) \geq 0 \quad (9)$$

From (9), the proposed *NDVSI* will be expressed as follows:

$$NDVSI = V_i^2 \sin^2(\theta - \delta + 45^\circ) - 2\sqrt{2}Z(P_j + Q_j) \sin(\theta + 45^\circ) \geq 0 \quad (10)$$

The values of *NDVSI* are higher than zero for the stable operating system under normal load. The *NDVSI* values decrease to zero when the system is exposed to an instability phenomenon, like critical loading. The closer the *NDVSI* value is to zero, the higher the risk of system voltage collapse.

2.3. Voltage Stability Assessment

In this context, the proposed *NDVSI* index is used to evaluate voltage stability under various load conditions in different distribution networks. At low load levels, the *NDVSI* values are significantly lower than the stability threshold, indicating that the system operates with a high loading margin and maintains good voltage stability. As the load increases, the *NDVSI* gradually decreases, with the index reaching zero as the load approaches its maximum capacity, signaling the loss of voltage stability. To validate the performance of the suggested *NDVSI*, it is compared with several widely recognized stability indices, including *SI* [37], *SI* [38], and *SI* [39]. This comparison ensures that the *NDVSI* offers an accurate and reliable voltage stability assessment, contributing to more effective management of power distribution systems and improved system reliability. The proposed *NDVSI* provides a distinct advantage by effectively identifying critical loading conditions in each scenario, a capability that conventional stability indices lack.

2.4. Indicating the Suitable Size and Siting of DGs

Figure 3 illustrates the strategy employed to address the problem of distributed generation (DG) siting and sizing within radial distribution networks based on the *NDVSI*. The proposed approach uses analytical methods alongside a systematic search technique to optimize DG placement and sizing, enhancing voltage stability by improving voltage profiles and minimizing energy losses. The following sequence of actions summarizes the step-by-step process used to identify the most suitable locations and ratings for DG units, ensuring improved system performance and reliability:

1. Inject the load bus by the DG at a time.
2. Execute load flow and analyze the obtained results.
3. Compute the proposed index and find $\sum NDVSI$.
4. Check all the load buses (PQ), excluding the slack bus.
5. Rank the $\sum NDVSI$ according to the highest improvement.
6. Select the optimal placement and size of the DG at the candidate bus, taking into account the weak nodes and their neighboring buses in terms of voltage stability.
7. Gradually increase the DG size, ensuring the voltage at the DG-installed bus does not exceed 1.05 p.u. Adjust and resize each unit accordingly using this approach for multiple DG units.

8. The analytical method and search technique are utilized to obtain the maximum stability margin (max $\sum NDVSI$) and minimum total energy loss (min $\sum P_{loss}$) for each DG size, i.e., choose the *NDVSI* with the highest value and the total loss with the lowest value.
9. Modify the DG using different power factors.
10. For validation, compare the findings obtained from the proposed approach with those from existing research in the literature.
11. Record the placement and sizing of DG units, and assess the improvements resulting from their integration into the system, such as voltage profile, power loss reduction, energy cost savings, stability enhancement $\sum NDVSI$, DG power cost, the percentage decrease in power supplied to the system from the substation, the cost of power provided from DGs, and the percentage of decrease in power supplied to the system from the substation.

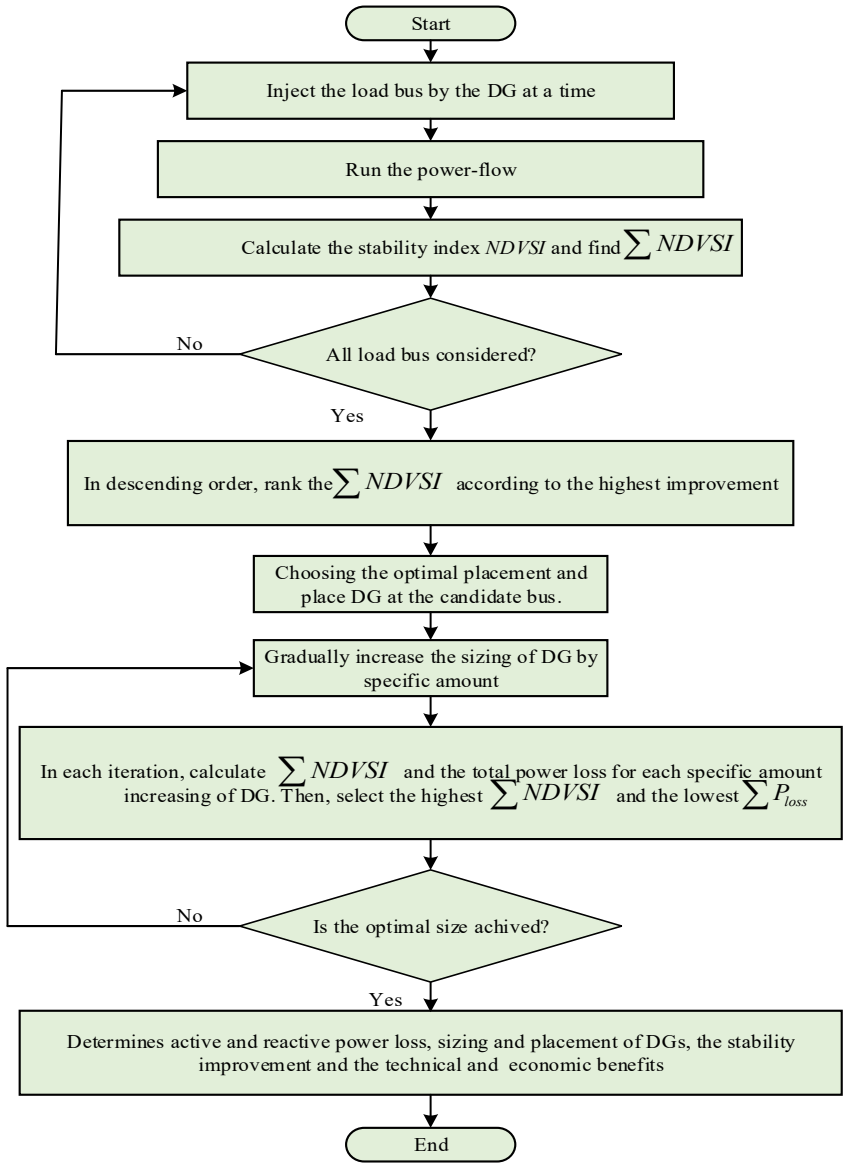


Figure 3. Flowchart for determining the optimal placement and sizing of DGs.

2.5. Cost of Energy Loss and Cost of Active and Reactive Power of DGs

The energy loss cost (ELC) and the costs associated with the active and reactive power components of DGs are determined using the following equations.

- Energy loss cost (ELC)

  The annual energy loss cost ($AELC$) is expressed as follows:

$$AELC = (TPL) \times (E_c \times T_d) \tag{11}$$

E_c illustrates the energy cost (USD/kWh), TPL represents the total power loss, and T_d shows period (h), where E_c = 0.06 USD/kWh and the time duration for a year is T_d = 8760 h.

- Cost of Active and Reactive Power Generation from DG

  The cost characteristics of DG are selected according to the data provided in [41].

$$C(P_{dg}) = aP_{dg}^2 + bP_{dg} + c \quad \text{USD/h} \tag{12}$$

The cost parameters are specified as follows: a = 0, b = 20, and c = 0.25. The cost of reactive power generated by the DG is computed based on the maximum complex power output from the DG, as detailed in [30].

$$C(Q_{dg}) = w \times \left[\text{cost}(S_{g\max}) - \text{cost}\left(\sqrt{S_{g\max}^2 - Q_{g\max}^2}\right)\right] \quad \text{USD/h} \tag{13}$$

where $S_{g\max} = P_{g\max}/pf$, $P_{g\max} = 1.1 \times P_{dg}$, and $w = 0.05 - 0.1$. In this article, the factor w is set at 0.1.

3. Case Studies and Simulation Analysis

3.1. Stability Assessment of IEEE 12-, 33-, and 69-Bus Under Different Load Conditions

This section tests the applicability and efficiency of the suggested *NDVSI* in the voltage stability assessment of three electric networks (IEEE 12, 33, and 69 bus). This work utilizes these systems as standard test cases. These systems are commonly adopted in distribution network studies due to their well-known structure, open-access datasets, and diversity in network scale. Their frequent application in prior research enables effective performance validation of the proposed approach and facilitates result comparison under different network configurations.

Figure 4 illustrates the topology of the IEEE 12-bus distribution system. It comprises 12 buses, with bus 1 serving as the reference (slack) bus and the remaining 11 as load buses. The total active power demand is 435 kW, while the total reactive power demand is 405 kVAr. The system is modeled using a 100 MVA apparent power base and a base voltage of 11 kV. Detailed line and bus data are provided in the Data Availability section at the end of the manuscript.

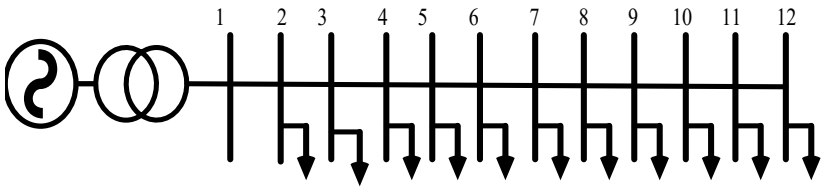


Figure 4. A line diagram of the IEEE 12-bus benchmark system.

The structure of the IEEE 33-bus radial distribution network is depicted in Figure 5. This system consists of 33 buses, with bus 1 as the slack bus and the remaining 32 as load buses. The total active and reactive power demands are 3.715 MW and 2.3 MVAr, respectively. The system is modeled using a base voltage of 12.66 kV and a base apparent power of 100 MVA. Detailed bus and line data are provided in the Data Availability section.

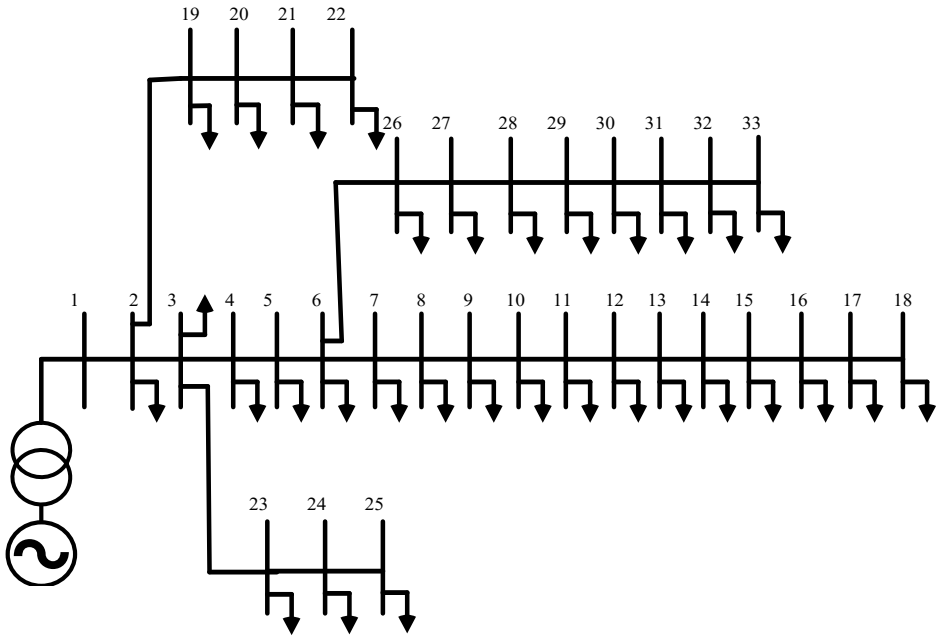


Figure 5. A line diagram of the IEEE 33-bus benchmark system.

Figure 6 presents the layout of the IEEE 69-bus radial distribution system. It comprises 69 nodes, where bus 1 is defined as the reference (slack) bus, and the remaining 68 buses are designated for load consumption. The cumulative power demand across the network amounts to approximately 3.8019 MW of active power and 2.6946 MVAr of reactive power. The system operates on a 12.66 kV base voltage and a 100 MVA base power. The Data Availability section provides complete details of the bus and line parameters and related variables.

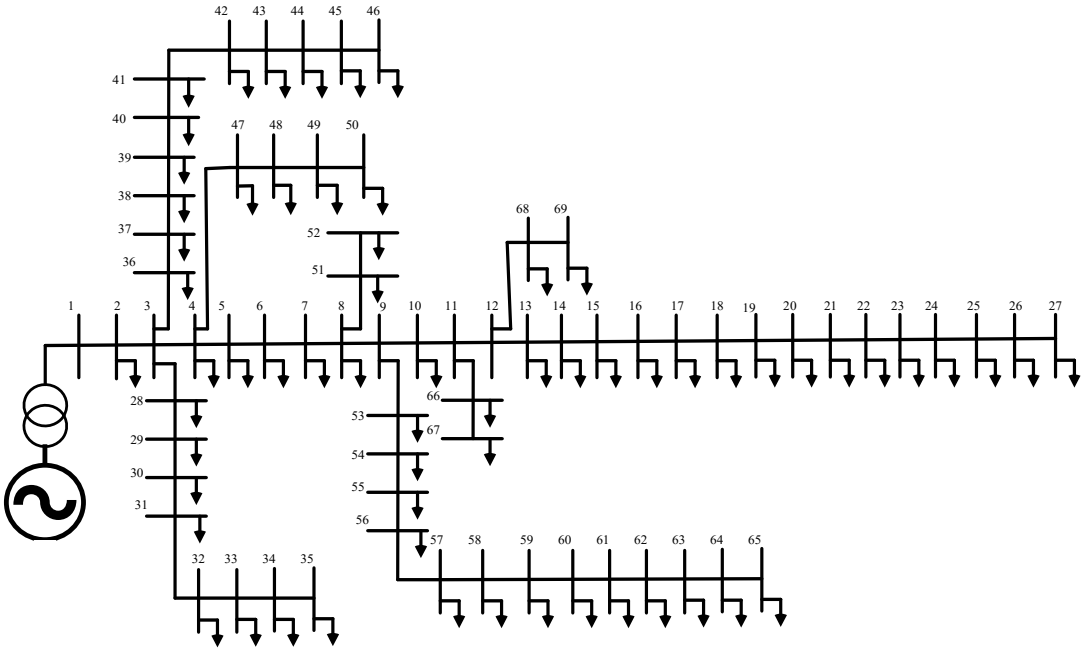


Figure 6. A line diagram of the IEEE 69-bus benchmark system.

The feasibility and applicability of the proposed indicator have been extensively examined by comparing it with conventional voltage stability indices across multiple IEEE benchmark systems, including the 12-bus, 33-bus, and 69-bus radial distribution networks. These evaluations were conducted under a variety of system configurations and operating

conditions to ensure a comprehensive assessment of its behavior and reliability in different distribution scenarios.

3.1.1. Stability Analysis of IEEE 12-, 33-, and 69-Bus Test Networks at Base Load Condition

In this operating case, the stability of IEEE 12-bus, 33-bus, and 69-bus systems is tested during normal load conditions without increasing the load. The results have been tabulated in Table 2.

Table 2. Stability indices for base state loading of IEEE 12-, 33-, and 69-bus test systems.

Model	Line	Bus	*NDVSI*	*SI* [37]	*SI* [38]	*SI* [39]
IEEE 12 bus	3–4	4	0.8057	0.9241	0.4724	0.9404
	6–7	7	0.7886	0.8626	0.4617	0.8677
	8–9	9	0.6690	0.8048	0.4410	0.8188
	10–11	11	0.7349	0.7933	0.4446	0.7945
	11–12	12	0.6784	0.7926	0.4449	0.7929
IEEE 33 bus	4–5	5	0.8336	0.8775	0.4612	0.8913
	6–7	7	0.6872	0.8006	0.4441	0.8067
	11–12	12	0.6700	0.7098	0.4199	0.7121
	19–20	20	0.9762	0.9719	0.4894	0.9790
	29–30	30	0.7616	0.7218	0.4215	0.7275
	32–33	33	0.8014	0.7053	0.4196	0.7057
IEEE 69 bus	4–5	5	0.9902	0.9961	0.4982	0.9977
	8–9	9	0.8619	0.9128	0.4766	0.9149
	26–27	27	0.7296	0.8365	0.4573	0.8365
	37–38	38	0.9929	0.9984	0.4994	0.9987
	53–54	54	0.8475	0.8904	0.4687	0.8964
	59–60	60	0.6495	0.7154	0.4183	0.7234

The application results show the stability conditions of the systems for a few buses because of space restrictions. Figures 7–9 show the remaining proposed stability index values. The analysis confirms the stability of all three systems, as none of the *NDVSI* values exhibit proximity to zero, indicating a safe margin from the critical instability threshold. The existing stability indices confirm that the systems are stable, as all index values are far from the critical threshold (0.0). Figure 7 shows the values of the proposed *NDVSI* for the IEEE 12-bus system under base case loading. It is observed that the *NDVSI* reaches its minimum values at buses 8, 9, and 10, with bus 9 having the lowest value. These low *NDVSI* values indicate that these buses have a reduced voltage stability margin.

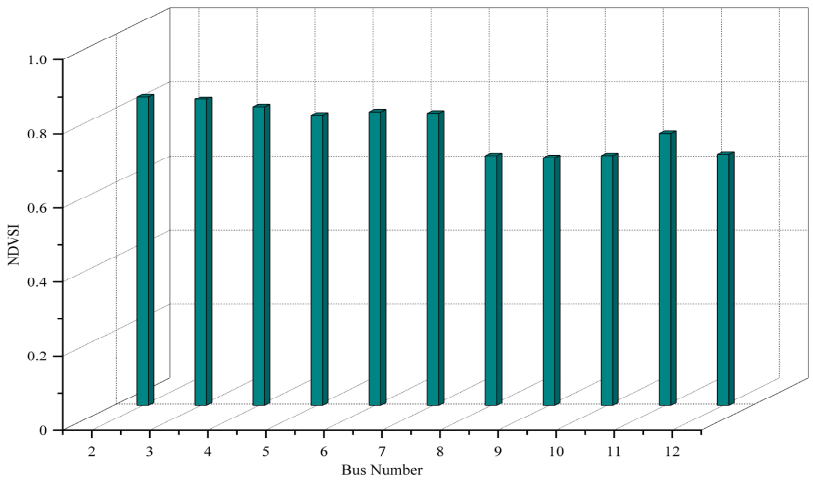


Figure 7. *NDVSI* for IEEE 12-bus test system at the base loading case.

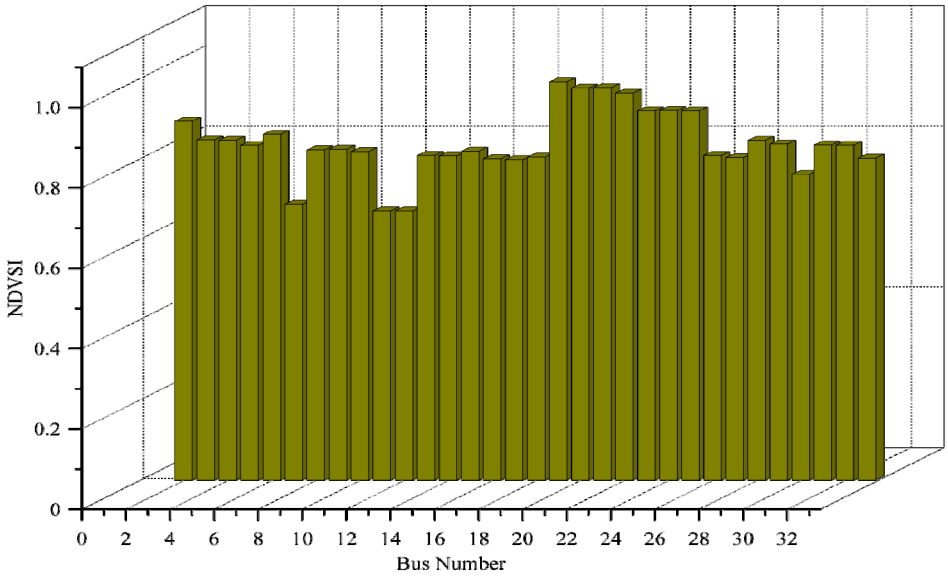


Figure 8. *NDVSI* for IEEE 33-bus test system at the base loading case.

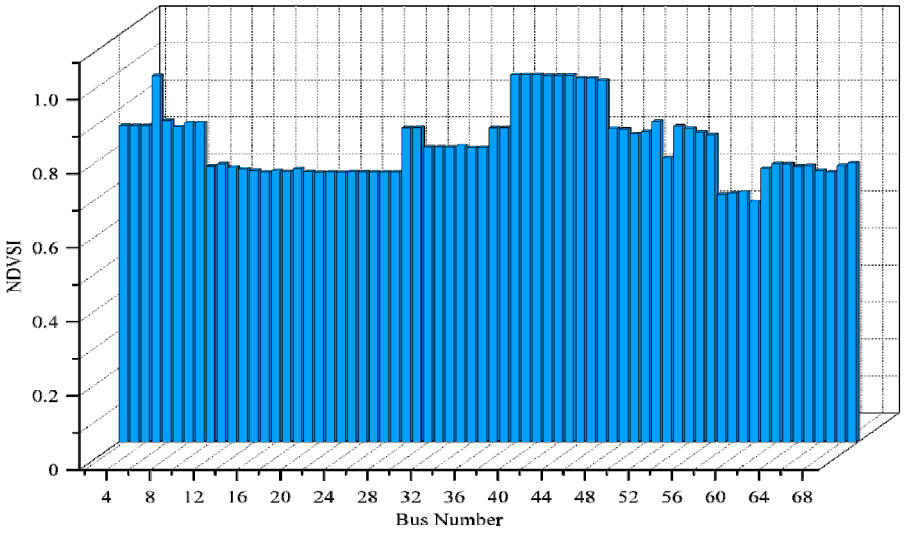


Figure 9. *NDVSI* for IEEE 69-bus test system at the base loading case.

Figure 8 presents the *NDVSI* values for the IEEE 33-bus system under base case loading. The indicator shows low values at bus 7, located between buses 6 and 8, as well as at buses 11 and 12, between buses 10 and 13. A low value is also observed at bus 30. These regions with low *NDVSI* values indicate weak voltage stability. A bus is considered stable when its *NDVSI* value is significantly above the critical threshold (0.0), indicating a safer margin from voltage collapse.

The *NDVSI* values shown in Figure 9 represent the stability status of the IEEE 69-bus system under normal loading conditions. It is observed that buses 10 to 27 and buses 55 to 61 exhibit the lowest *NDVSI* values in the network. These areas are considered the weakest in the system, as the low indicator values reflect a reduced voltage stability margin.

As a result, the proposed index can be utilized as a promising tool for assessing voltage stability in distribution systems by indicating how close or far the system is from voltage collapse in any part of the network. When the index value at any point approaches the critical limit (zero), operators can implement corrective actions such as load reduction or capacitor bank switching to enhance stability and prevent collapse. The following case studies demonstrate how *NDVSI* values respond under conditions of substantial load increase.

3.1.2. Voltage Stability Evaluation of IEEE 12-, 33-, and 69-Bus Test Systems Under High Loading Conditions

In this operation stage, the systems are examined during different heavy loadings as follows.

IEEE 12 bus: As presented in Table 3, the *NDVSI* values tend to move closer to the instability threshold (0.0) due to the high levels of electric power demand. The *NDVSI* results are supported by the *SI* values in [37], which similarly approach the critical threshold under maximum loading conditions. Nevertheless, the *NDVSI* demonstrates higher accuracy in assessing voltage stability. The stability indices *SI* [38] and *SI* [39] do not reach the stability limits because of the high reactive power demand at node 9. It is also seen that the proposed indicator diagnoses the voltage collapse points under several power factors during heavy apparent power loadings at node 9. The other existing indices verify the capability of the *NDVSI* since they also diagnose the instability phenomenon under these loadings. Nevertheless, the *NDVSI* is nearer to the stability threshold than the other indices. The critical bus (CB) and critical line (CL) under heavy loadings are also identified.

Table 3. Stability indices for critical loading cases in a single bus of IEEE 12-, 33-, and 69-bus test systems.

Model	Load	Bus	CB	CL	*NDVSI*	*SI* [37]	*SI* [38]	*SI* [39]
IEEE 12 bus	P = 2.98 MW	6	5	4–5	0.0354	0.0368	0.0376	0.1647
	Q = 1.874 MVAr	9	9	8–9	0.0781	0.0682	0.1241	0.1424
	S = 1.31 MVA and pf = 0.707	9	9	8–9	0.0420	0.0391	0.0550	0.0966
	S = 1.25 MVA and pf = 0.93	9	9	8–9	0.0309	0.0361	0.0425	0.0891
IEEE 33 bus	P = 11.099 MW	22	20	19–20	0.0003	−0.0115	0.0477	0.4042
	Q = 13.67 MVAr	25	25	24–25	0.0270	−0.0125	0.0556	0.1122
	S = 12.42 MVA and pf = 0.765	6	6	5–6	0.0004	0.0111	0.0229	0.1492
	S = 12.646 MVA and pf = 0.95	6	6	5–6	0.0010	−0.0008	0.0251	0.1441
IEEE 69 bus	P = 5.98 MW	15	15	14–15	0.0491	0.0453	0.0722	0.0780
	Q = 21.4 MVAr	43	41	40–41	0.0008	−0.0333	0.0382	0.3277
	S = 18.93 MVA and pf = 0.77	43	41	40–41	0.0000	−0.0011	0.0350	0.3454
	S = 19.914 MVA and pf = 0.93	43	41	40–41	0.0000	−0.0013	0.0438	0.3550

IEEE 33 bus: Four different critical loadings are applied at various buses in the IEEE 33-bus system to evaluate the efficacy of the proposed index. The findings in Table 3 show that the critical active and reactive loadings at nodes 22 and 25 make the values of the suggested indicator reach 0.0003 and 0.0270 for the branches 19–20 and 24–25, respectively. This means that these branches are critical, and voltage collapse, without a doubt, occurs during any slight disturbance.

It is evident that *SI* [38] corroborates the results, as it detects the same critical branches. However, the proposed index is the one that is closest to the stability limit (0.0). Interestingly, *SI* [37] exceeds the stability limit (zero) and takes on negative values, suggesting the system has already experienced a collapse. On the other hand, *SI* [39] still diagnoses the system as stable at the critical loading. Under critical complex power loading with varying power factors at node 6, the suggested index yields nearly zero values, indicating proximity to collapse. In contrast, *SI* [37] falls below the stability limit, reaching a value of −0.0008, which indicates that the system has already undergone voltage collapse. *SI* [38] proves the results of *NDVSI*, which also achieves the stability limit. *SI* [39] diagnoses the system as stressed, and its values fail to reach the stability limit (zero).

IEEE 69 bus: The different loadings under different power factors are also applied in a large radial system to examine the proposed index practicability. Table 3 highlights

the efficiency of the suggested indicator in identifying voltage collapse points across various loading scenarios, as *NDVSI* consistently approaches zero under several operating conditions. Conversely, *SI* [39] reaches the stability threshold in only one case, as Table 3 shows its limited effectiveness. *SI* [38] verifies the findings of *NDVSI* since its values are also close to zero, while *SI* [37] passes the stability limit (zero) with negative values in three loading cases. Among all evaluated indices and under various loading conditions, *NDVSI* consistently exhibits values closest to the collapse point (zero).

3.1.3. IEEE 12-, 33-, and 69-Bus Test Systems at Multiple Power Loadings for Loading Margin (MVA) Identification

In this scenario, both active (P) and reactive power (Q) demands are simultaneously increased in fixed increments until the power flow solution fails to converge. This scenario is designed to evaluate how effectively the proposed *NDVSI* can identify the system's loading margin in MVA. The loading margins of the IEEE 12, 33, and 69 systems are computed and tabulated in Table 4, where λ represents the normal loading, and λ_{max} is the maximum loading. At maximum loading (critical loading), the proposed *NDVSI* and other stability indexes reach the stability threshold, whereas *SI* [39] fails to do so in the IEEE 69-bus system.

Table 4. Stability indices for multiple critical loading cases of IEEE 12-, 33-, and 69-bus test systems.

System	Loading Margin (MVA)	Critical Load	CB	CL	*NDVSI*	*SI* [37]	*SI* [38]	*SI* [39]
IEEE 12 bus	2.567	$\lambda_{\max} = 5.32\lambda$	9	8–9	0.0706	0.0619	0.0636	0.0710
IEEE 33 bus	10.54	$\lambda_{\max} = 3.412\lambda$	17 18	16–17 17–18	0.0243 0.0713	0.0333 0.0322	0.0847 0.0877	0.0361 0.0329
IEEE 69 bus	10.31	$\lambda_{\max} = 3.212\lambda$	57	56–57	0.0881	0.0704	0.0574	0.2027

The application results presented in Table 4 demonstrate the capability of the proposed *NDVSI* to assess voltage stability margins across various IEEE radial distribution systems. In the IEEE 12-bus system, the maximum loading reaches approximately 5.32 times the base loading case. The total load in the base case is S = 435 + j405 kVA (equivalent to 594.35 kVA), and the critical loading point is 3161.93 kVA, yielding a loading margin of 2567.58 kVA (2.567 MVA). Under this stressed condition, bus 9 and branch 8–9 are identified as the most critical.

The total load in the base case for the IEEE 33-bus system is S = 3.715 + j2.30 MVA or 4.369 MVA. The critical loading is observed at 3.412 times the base load, reaching 14.908 MVA and yielding a loading margin of approximately 10.54 MVA. The most vulnerable elements in this scenario are buses 17 and 18 and branches 16–17 and 17–18.

In the IEEE 69-bus system, the total load in the base case S = 3.8019 + j2.6946 MVA equivalent to 4.66 MVA. The system reaches its critical loading at 3.212 times the base load, corresponding to 14.9678 MVA, with an estimated loading margin of 10.31 MVA. Under this condition, bus 57 and branch 56–57 are identified as the most critical.

As a result, the proposed *NDVSI* proves to be a robust and promising tool for evaluating voltage stability margins in distribution power systems, offering valuable insight into system vulnerabilities and helping operators identify the most critical buses and lines under increasing load conditions.

3.2. Integration of Optimal DG Placement and Sizing in Radial Power Grids

The methodology for identifying the optimal sizing and placement of DG units is presented in the flowchart shown in Figure 3. The DG unit is inserted into each load bus to

identify the bus that provides maximum stability improvement using the proposed stability index (*NDVSI*). At the same time, the rating of DG gradually increases in each iteration for identifying the candidate buses, and the iteration is stopped when the minimum energy loss is obtained. The suggested approach aims to improve the radial power systems technically and economically. Technically, the system is enhanced by minimizing energy losses in the distribution lines, boosting the stability margin, increasing the load margin through an improved total stability index, enhancing the voltage profile, and strengthening system reliability by incorporating power from multiple sources. The systems are also improved economically by reducing the cost of energy losses and the cost of fuel by reducing the proportion of the power supplied from the substation. The impact of integrating the DGs on the economic aspect is analyzed from several aspects, such as the annual cost of losses and the energy cost of distributed generation, and compared in different operating scenarios. Ultimately, the proposed method is evaluated against various studies in the existing literature to demonstrate its effectiveness.

3.2.1. IEEE 12 Bus

As illustrated in Figure 7, bus 9 represents the weakest point in the IEEE 12-bus system, with neighboring buses 8 and 10 also demonstrating relatively low index values. Therefore, placing a DG at one of these locations is considered appropriate. Table 5 outlines four evaluation scenarios conducted on the IEEE 12-bus configuration, where system behavior is analyzed both in the absence and presence of distributed generation sources. The system is defined using a base value of 100 MVA for apparent power and 11 kV for voltage. When DG is not integrated, the active power loss amounts to 20.695 kW, and the reactive power loss is 8.04 kVAr. The active and reactive power supplied from the substation (APSFS and RPSFS) are 455.7 kW and 413 kVAr, respectively.

Table 5. Results from integrating DG into the IEEE 12-bus system.

Technical and Economic Analyses	No DG	With a Single DG at 1.0 pf	With a Single DG at 0.9 pf lag	With a Single DG at 0.74 pf lag	GUI [42], Single DG at 1.0 pf
	Case I	Case II	Case III	Case IV	
DG Placement	-	9	9	9	9
DG size (kVA)	-	235	304	315	234.9
Total P_{loss} (kW)	20.695	10.7587	4.4781	3.1400	10.774
Total Q_{loss} (kVAr)	8.040	4.1261	1.6369	1.1071	4.1261
$\sum NDVSI$	8.261	8.713	8.902	8.892	-
$V_{\min}$ (pu)@bus	0.9435@12	0.9835@7	0.9913@6	0.9908@6	0.9835@7
APSFS (kW)	455.7	210.80	165.9	205.0	N. A
RPSFS (kVAr)	413.0	409.10	274.1	194.2	N. A
Cost of P_{dg} (USD/h)	-	4.95	5.722	4.912	4.948
Cost of Q_{dg} (USD/h)	-	-	0.0548	0.1446	-
AELC (USD)	10,877.24	5654.77	2353.7	1650.38	5662.8
ELCS (USD)	-	5222.47	8523.6	9226.86	5214.43
RRCEL %	0%	48%	78.36%	84.83%	47.93%

Figure 7 shows that bus 9 is the weakest in the system. Also, inserting the DG unit into this bus provides a maximum total stability index (*NDVSI*). Therefore, the DG unit is placed at bus 9, and its rating is incrementally increased until the lowest energy loss is

achieved. When integrating DG into bus 9 with unity, 0.9, and 0.74 power factors, the real power loss decreases to 10.7587, 4.4781, and 3.140 (48%, 78.36%, and 84.83%), respectively, and the reactive power loss minimizes to 4.1261, 1.6369, and 1.1071, respectively.

In addition, the voltage stability margin has been improved, where the total *NDVSI* increases from 8.261 to 8.713, 8.902, and 8.892 in cases II, III, and IV, respectively. A noticeable reduction in power losses is observed when the DG operates with a lagging power factor, compared to its performance at a unity power factor. This is because the DG provides the load with the reactive power, which reduces the RPSFS. Installing the DG at bus 9 and operating it at its optimal power factor leads to a 55% reduction in active power and a 53% decrease in reactive power supplied from the substation, resulting in respective values of 205 kW and 194.2 kVAr. This signifies a notable increase in the stability and reliability of the radial distribution grid.

The annual energy loss cost (AELC) is minimized from USD 10,877.24 to USD 1650.38, i.e., the energy loss cost saving (ELCS) approaches USD 9226.86. In this case, the reduction rate in the cost of energy losses (RRCEL) reaches 84.84%. Table 5 depicts the findings of integrating DGs into the system under various scenarios. Inserting the DG into the system leads to a notable enhancement in the voltage profile. Figure 10 presents a comparison of the voltage profile across various cases, highlighting scenarios both with and without the inclusion of DG units. It is noted that the results achieved in [42] verify the proposed method when DG is integrated with the unity power factor at bus 9. Not Analyzed (N. A.) is used to indicate cases that were not examined in previous studies. The optimal DG size in [42] is approximately 234.9 kW, whereas the proposed method yields an optimal DG size of 235 kW.

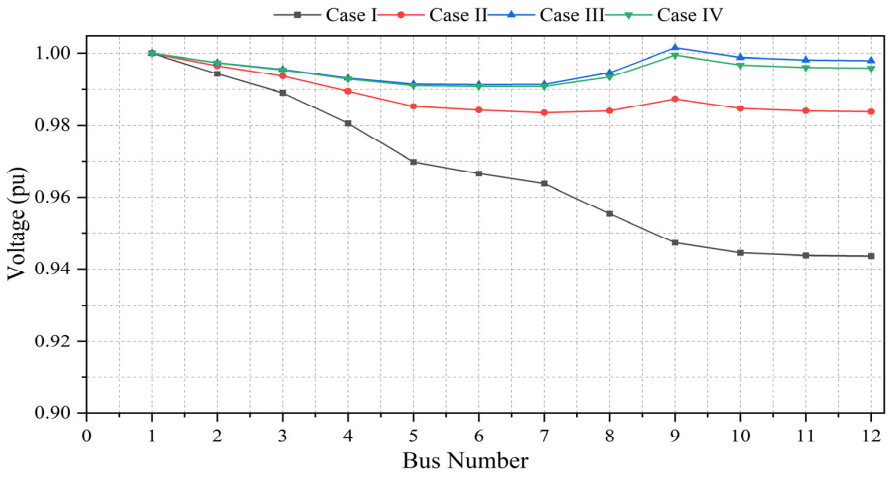


Figure 10. Voltage profile comparison with and without integrated DGs for the cases in Table 5.

3.2.2. IEEE 33 Bus

As shown in Figure 8, the lateral from bus 19 to bus 22 in the IEEE 33-bus system exhibits excellent voltage stability, indicating that there is no requirement for DG installation in this lateral. In the lateral spanning buses 6 to 18, Figure 8 shows that bus 7, along with its neighboring buses 6 and 8 and buses 11 to 13, exhibits low *NDVSI* values. In the lateral from bus 26 to 33, bus 30, and its adjacent buses also show low *NDVSI* readings. Similarly, in the 23–25 lateral, bus 24 presents a low index value. Therefore, the buses identified can be considered potential sites for DG placement, aiming to boost voltage stability and enhance the voltage profile by targeting locations with the highest stability margin and lowest energy loss. The sum of *NDVSI* approaches 26.8, and the minimum voltage is 0.9039. The operation of the radial IEEE 33-bus system is analyzed with and without integrating DG units in different cases, as depicted in Table 6. In case I, when no DG is incorporated

into the system, the active power loss totals 210.85 kW, and the reactive power loss amounts to 143.02 kVAr.

Table 6. Results from integrating DG into the IEEE 33-bus system.

Technical and Economic Analyses	No DG	With a Single DG at 1.0 pf	With a Single DG at 0.9 pf lag	With Double DGs	With Triple DGs
	Case I	Case II	Case III	Case IV	Case V
DG Placement	-	6	6	13 and 30	13, 24 and 30
DG size (kVA), *pf*@bus	-	2589	3011	957.55, 0.908@13 1514.7, 0.714@30	870.18, 0.905@13 1176.2, 0.897@24 1445.37, 0.713@30
Total P_{loss} (kW)	210.85	110.90	70.790	28.57	11.73
Total Q_{loss} (kVAr)	143.02	81.67	56.716	20.33	9.76
$\sum NDVSI$	26.80	28.44	29.05	29.967	30.11
$V_{\min}$ (pu)@bus	0.9039@18	0.9425@18	0.9566@18	0.9802@25	0.9919@8
APSFS (kW)	3925.8	1236.9	1075.9	1791.6	854.10
RPSFS (kVAr)	2443.0	2381.7	1044.2	860.3	405.80
Cost of P_{dg} (USD/h)	-	52.03	54.45	39.54	58.20
Cost of Q_{dg} (USD/h)	-	-	0.5423	0.9200	1.0985
AELC (USD)	110,376	58,289	37,207.224	14,979.6	6165.3
ELCS (USD)	-	52,087	73,168.80	95,396.4	104,210.7
RRCEL %	0.0%	47.2%	66.3%	86.43%	94.42%

The active and reactive power supplied from the substation (APSFS and RPSFS) are 3925.8 kW and 2443 kVAr, respectively. The annual energy loss cost (AELC) is USD 110,376. The load buses of IEEE 33-bus are examined to choose the bus that gives the maximum total stability index (*NDVSI*) due to the injection of the DG unit. DG output is progressively increased at the chosen location to determine the point of minimal system loss. DG installation is performed at bus 6, considering scenarios with unity and 0.9 power factor levels. Using a DG at unity power factor brings the system loss down to 110.9 kW, whereas operating it at a 0.9 power factor further lowers the loss to 70.79 kW. This means that the reduction rates in the cost of energy losses (RRCEL) are 47.2% and 66.3% due to the integration of DG at bus 6 with unity and 0.9 power factors, respectively. The annual savings in energy loss cost are USD 52,087 and USD 73,168.80 because of integrating DG at bus 6 with unity and 0.9 power factors, respectively.

It is noted that the total stability index (*NDVSI*) increases from 26.8 to 28.44 and 29.05 in cases II and III, respectively. System reliability is enhanced as both the active and reactive power drawn from the substation (APSFS and RPSFS) are significantly reduced. The DG working at a lagging power factor achieves greater reductions in APSFS and RPSFS than the unit working at a unity power factor. Cases IV and V in the table represent the system with multiple DG units at different power factors. After indicating the candidate buses for DG locations, the power factors of DG units have been changed under many iterations to get the minimum power loss. It is noted that the power losses are minimized to 28.57 kW and 11.73 kW when inserting 2 DG units and 3 DG units, respectively.

The stability margin is highly improved since the total *NDVSI* increases to 29.967 and 30.11 in cases IV and V, respectively. The reliability of the system is increased due to the multiple integration of DG units into the system. It is noted that the APSFS and RPSFS

reduced from 3925.8 kW and 2443.0 kVAr to 854.10 kW and 405.80 kVAr, respectively, when three DG units are inserted into the system. In the absence of distributed generators, the network relies entirely on the substation to supply both real and reactive power. Integrating three DGs in appropriate sizes and locations results in a 78.47% reduction in the reliance on the substation for real power and a 67.2% decrease in the need for reactive power from the substation. In this case, the RRCEL is 94.42%, while the RRCEL with 2 DG units is 86.43%. The results show that the annual energy loss cost savings (ELCS) are USD 95,396.4 and USD 104,210.7 in cases IV and V, respectively. It means that the reduction rates in the cost of energy losses (RRCEL) are 86.43% and 94.42% in cases IV and V, respectively. Incorporating DG units into the system significantly enhances the voltage profile. Figure 11 represents the voltage profile during the five different cases shown in Table 6.

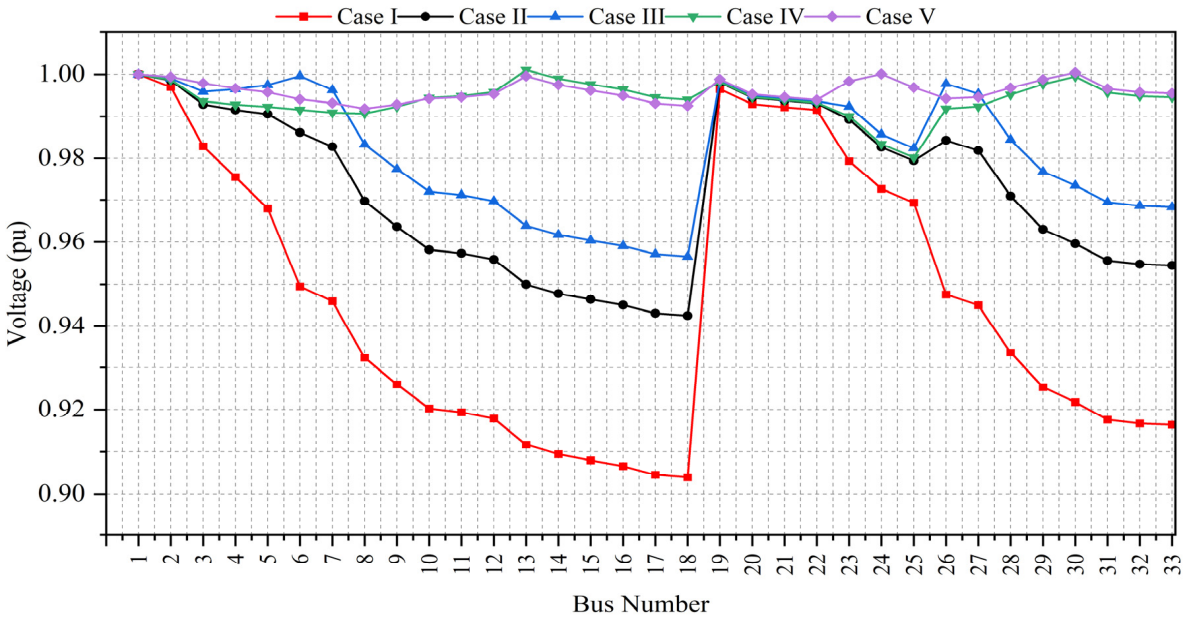


Figure 11. Voltage profile comparison with and without integrated DGs for the cases in Table 6.

The effectiveness of the suggested approach is validated by comparing it with existing methods, as presented in Table 7. N. A. indicates cases that were not analyzed in the existing studies. When a single DG with a 0.9 power factor is applied, the suggested approach minimizes power losses to 70.79 kW. The sensitivity approach (SA) [30] reduces the power loss to 112.78 kW when a DG of 1200 kW is inserted into bus 16. On the other hand, the dragonfly algorithm (DFA) method inserted the DG of 3073.5 kW with 0.9 pf at bus 9 as the optimal sizing.

The proposed approach selects the DG of 3011 kW as the optimal size, which is lower than the DG sizing in the DFA method. It is noted that the proposed method inserts DG of 3011 kW while the DFA inserts DG of 3073 kW, and the power loss reduction is almost the same in the two methods. Thus, the DFA did not yield the precise optimal sizing for the DG units. Additionally, the proposed method is compared with the particle artificial bee colony algorithm (PABC) [43] and the backtracking search optimization algorithm (BSOA) [15] when three DG units are integrated into the system. Table 7 highlights that the proposed approach achieves a notably greater reduction in system power losses compared to both the PABC and BSOA techniques. The existing studies also did not analyze (N. A) the APSFS and RPSFS. The comparison, technically and economically, is shown in Table 7.

Table 7. Comparison of the proposed method results with existing studies for the IEEE 33-bus.

Technical and Economic Analyses	Single DG at 0.9 pf			Triple DGs with Different pf		
	Proposed Method	**SA [30]**	**DFA [14]**	**Proposed Method**	**PABC [43]**	**BSOA [15]**
DG Placement	6	16	6	13, 24, and 30	12, 25, and 30	13, 29, and 31
DG size (kVA), *pf*@bus	3011	1200	3073.5	870.18, 0.905@13 1176.2, 0.897@24 1445.37, 0.713@30	1014, 0.85@12 960, 0.85@25 1363.5, 0.85@30	698, 0.86@13 402, 0.71@29 658, 0.70@31
Total P_{loss} (kW)	70.790	112.78	70.86	11.73	15.91	29.65
Total Q_{loss} (kVAr)	56.716	77.45	56.77	9.76	N. A	21.23
$\sum NDVSI$	29.05	-	-	30.11	-	-
V_{min} (pu)	0.9566	0.937	0.9566	0.9919	0.9889	0.979
APSFS (kW)	1075.9	2845.97	N. A	854.10	N. A	N. A
RPSFS (kVAr)	1044.2	1919.96	N. A	405.80	N. A	N. A
Cost of P_{dg} (USD/h)	54.45	21.85	55.57	58.20	57.50	27.176
Cost of Q_{dg} (USD/h)	0.5423	0.2161	0.554	1.0985	1.5464	0.7284
AELC (USD)	37,207.224	59,277.17	37,244.02	6165.3	8362.3	15,584.04
ELCS (USD)	73,168.80	51,098.8	73,131.98	104,210.7	102,013.7	94,791.96
RRCEL %	66.3%	46.30%	66.25%	94.42%	92.42%	85.88%

3.2.3. IEEE 69 Bus

In the lateral spanning buses 10 to 27 of the IEEE 69-bus system, Figure 9 indicates that these buses exhibit low *NDVSI* values. Similarly, in the segment extending from bus 53 to bus 65, Figure 9 shows buses 57 to 61 have low voltage stability index values. Consequently, deploying distributed generation at these particular points has the potential to optimize network stability and efficiency. Figure 6 illustrates the schematic of the IEEE 69-bus network. A base voltage of 12.66 kV and a base apparent power of 100 MVA are adopted for system analysis. The results in Table 8 depict the technical and economic analysis with and without DG units. Under base loading conditions, case I examines the system without distributed generation (DG), yielding active power losses of 224.978 kW and reactive power losses of 102.15 kVAr. $\sum NDVSI$ is 55.02 during the base loading case, and the annual energy loss cost (AELC) is USD 118,248.43.

The system is also tested by integrating DG in different cases (cases II, III, IV, and V), as shown in Table 8. When a single DG unit is placed at bus 61, the power losses decrease to 83.2 kW and 27.94 kW for unity and 0.9 power factors, respectively. The reduction in power losses is significantly greater when the DG functions at a lagging power factor (case III) compared to when it runs at a unity power factor (case II).

Figure 12 shows a significant improvement in the voltage profile in case III compared to case II. It is noticed that the APSFS in case II is reduced by 50% of APSFS in case I, while the RPSFS is only reduced by 2.2% of RPSFS in case I. On the other hand, the APSFS and RPSFS in case III are reduced by 54.22% and 37.63% of APSFS and RPSFS in case I, respectively. It indicates that the DG at a lagging power factor minimizes the RPSFS far better than the DG with a unity power factor. The total of *NDVSI* is improved to 56.85 and 57.23 in cases II and III, respectively. The results show that the annual energy loss cost savings (ELCS) are USD 74,518.51 and USD 103,561.6 in cases II and III, respectively. It

means that the reduction rates in the cost of energy losses (RRCEL) are 63.02% and 87.6% in cases II and III, respectively.

Table 8. Results from integrating DG into the IEEE 69-bus system.

Technical and Economic Analyses	No DG	With a Single DG at 1.0 pf	With a Single DG at 0.9 pf lag	With Double DGs	With Triple DGs
	Case I	Case II	Case III	Case IV	Case V
DG Placement	-	61	61	17 and 61	11, 17, and 61
DG size (kVA), *pf*@bus	-	1871	2217	635.14, 0.834@17 2136.63, 0.814@61	608.73, 0.812@11 454, 0.835@17 2057.6, 0.814@61
Total P_{loss} (kW)	224.978	83.20	27.943	7.200	4.20
Total Q_{loss} (kVAr)	102.15	40.53	16.45	8.045	6.76
$\sum NDVSI$	55.02	56.85	57.23	57.99	58.20
V_{min} (pu)@bus	0.9092@65	0.9683@27	0.9724@27	0.9942@50	0.9943@50
APSFS (kW)	4026.9	2014.1	1834.5	1549.1	1257.7
RPSFS (kVAr)	2796.7	2735.1	1744.4	1112.6	901.4
Cost of P_{dg} (USD/h)	-	37.67	40.156	45.87	51.72
Cost of Q_{dg} (USD/h)	-	-	0.3994	0.8971	1.433
AELC (USD)	118,248.43	43,729.9	14,686.8	3784.32	2207.52
ELCS (USD)	-	74,518.51	103,561.6	114,464.11	116,040.91
RRCEL %	0%	63.02%	87.6%	96.80%	98.13%

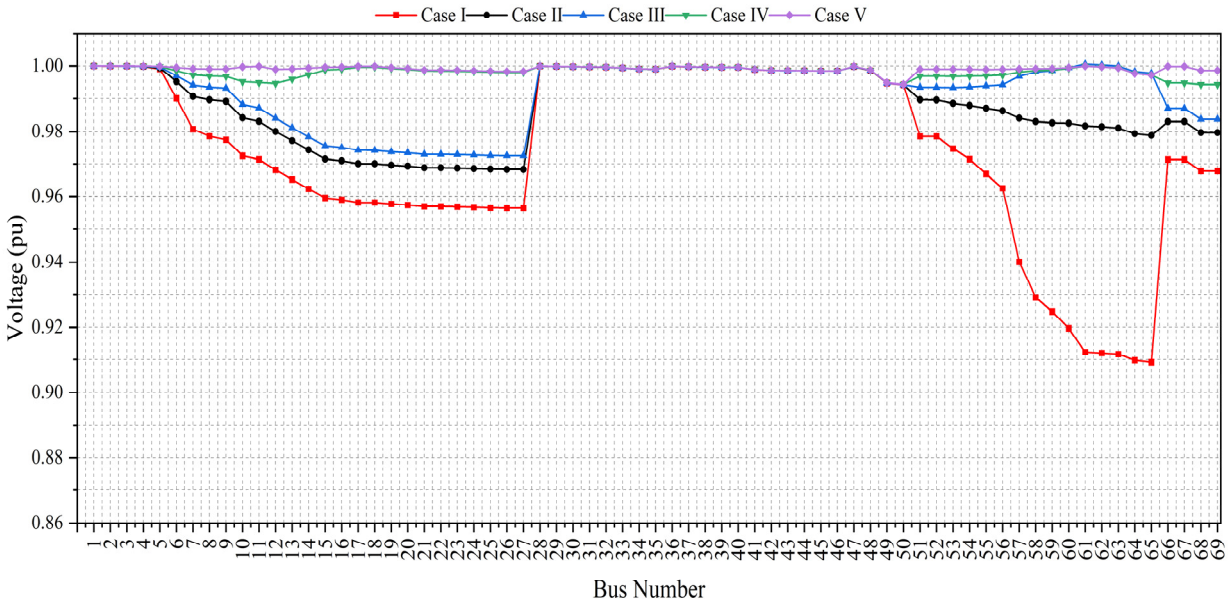


Figure 12. Voltage profile comparison with and without integrated DGs for the cases in Table 8.

The system is also tested by integrating double and triple DG units (cases IV and V). Cases IV and V reduce total power losses to 7.20 kW and 4.2 kW, respectively. It is noted that the total energy loss is greatly minimized by expanding the integration of DG units with lagging power factors.

The technical and economic analyses are tabulated in Table 8. The reduction rate in the cost of energy loss (RRCEL) reaches 98.13% due to integrating triple DGs at nodes 11,

17, and 61, while the RRCEL reaches 96.80% due to integrating two DG units at nodes 17 and 61. The annual energy loss cost savings (ELCS) are USD 114,464.11 and USD 116,040.91 in cases IV and V, respectively. The reliability of the grid is highly improved with triple integrating DGs, where the APSFS and RPSFS are minimized from 4026.9 kW and 2796.7 kVAr to 1257.7 kW and 901.4 kVAr, respectively. Without DGs, the network relied on active and reactive power from the substation by 100%. With the penetration of three DGs into appropriate sizes and sites of the system, the network dependence on active power and reactive power from the substation is 31.30% and 32.23%, respectively. The stability margin has also improved since the total *NDVSI* has increased from 55.02 to 58.10. Figure 12 depicts the voltage profile for both scenarios, with and without the integration of DG units, for the five cases outlined in Table 8. The voltage profile improvement is notably greater when three DG units are used than in the other scenarios.

The outcomes of the proposed approach are also contrasted with those from previous studies, including voltage sensitivity index (VSI) [30], hybrid optimization [44], and particle swarm optimization (PSO) [44], as presented in Table 9. The proposed method identifies node 61 as the optimal location for placing a single DG. The DG of 2217 kW installed at node 61 reduces the energy loss to 27.943 kW, whereas the VSI method [30] reduces the energy loss to 65.45 kW when the DG is located at bus 65. This highlights the significant impact of DG location on the system's technical performance and economic efficiency. On the other hand, the suggested approach minimizes the power loss by 98.13% when the triple DGs are inserted at nodes 11, 17, and 61. In contrast, the hybrid and PSO methods minimize the power loss to 98.08% and 97.95%, respectively. The nominated buses for integrating DG units into the system in the proposed method are 11, 17, and 61, while the nominated buses in hybrid and PSO are 18, 61, and 66 and 11, 18, and 61, respectively. The remaining technical and economic analyses are shown in Table 9 in detail. It is noted that the proposed approach improves the system technically and economically, with significantly better results than the existing methods.

Table 9. Comparison of proposed method results with existing studies for the IEEE 69 bus.

Technical and Economic Analyses	Proposed Method		VSI [30]	Hybrid [44]	PSO [44]
	One DG at 0.9 pf lag	Triple DGs	One DG at 0.9 pf lag	Triple DGs	Triple DGs
DG Placement	61	11, 17, and 61	65	18, 61, and 66	11, 18, and 61
DG size (kVA), *pf*@bus	2217	608.73, 0.812@11 454, 0.835@17 2057.6, 0.814@61	1750	480, 0.77@18 2060,0.83@61 530, 0.82@66	600, 0.83@11 460, 0.81@18 2060, 0.81@61
Total P_{loss} (kW)	27.943	4.20	65.45	4.30	4.61
Total Q_{loss} (kVAr)	16.45	6.76	35.625	N. A	N. A
$\sum NDVSI$	57.23	58.10	-	-	-
V_{min} (pu)	0.9724	0.9943	0.9693	N. A	N. A
APSFS (kW)	1834.5	1257.7	2415.28	N. A	N. A
RPSFS (kVAr)	1744.4	901.4	2032.92	N. A	N. A
Cost of P_{dg} (USD/h)	40.156	51.72	31.75	51.03	51.534
Cost of Q_{dg} (USD/h)	0.3994	1.433	0.3160	1.3840	1.0357
AELC (USD)	14,686.8	2207.52	34,400.5	2260.08	2423.02
ELCS (USD)	103,561.6	116,040.91	83,847.91	115,988.35	115,825.41
RRCEL %	87.6%	98.13%	70.9%	98.08%	97.95%

4. Conclusions

This study presents the novel distribution voltage stability index (*NDVSI*) for two main purposes. The first is to assess the voltage stability in different radial power distribution grids under various loading conditions. The application findings demonstrate the clear advantage of the proposed index in accurately identifying voltage collapse points across various critical loading conditions, including active, reactive, and apparent power loadings. Moreover, the results highlight the ability of the proposed index to effectively pinpoint the critical branches and vulnerable buses within the systems under severe loading conditions. The proposed index effectively and precisely calculates various radial power systems' loading margins (MVAs). The results obtained from different operating loadings and systems clearly demonstrate the accuracy and effectiveness of the suggested approach in comparison to other existing approaches. This is because the suggested index considers all the distribution line parameters, excluding the shunt line admittance, which is negligible in distribution systems. The proposed method incorporates the voltage angle difference, a factor often overlooked by existing indices.

The second objective of the proposed approach is to determine the suitable size and location for DG units in radial distribution networks. The results from the application to three IEEE radial distribution systems clearly demonstrate the efficacy of the proposed method in facilitating improved planning for the optimal sizing and placement of DG units. The proposed method improves the system technically and economically. The technical improvements include a reduction in power losses and enhancements in the voltage profile, stability margin, and overall reliability. Economically, the method decreases annual energy loss costs and reduces the cost of power generation from the substation by lessening the system's reliance on a single power source (the substation). The application results show the annual energy cost savings due to the integration of DG units. Integrating DG units at lagging power factors improves the system better than the DG at unity power factors. The system is significantly improved by increasing the penetration of DG units into the systems. The suggested method has been benchmarked against existing studies to assess its feasibility. In several instances, the comparison results illustrate the superior functionality of the method in determining the optimal placement and sizing of DG units.

The proposed *NDVSI* effectively assesses voltage stability and guides DG placement in radial distribution systems. However, it assumes static loads and radial topology, without accounting for dynamic behaviors or uncertainties. Future work will address these limitations to improve robustness and applicability.

5. Future Works

The proposed *NDVSI* has low input variables and parameters input, and it effectively assesses the stability of radial distribution systems, including indicating the optimum location of DGs. The future work can be implemented using the proposed index as follows:

- In future work, Monte Carlo simulation can be applied alongside the proposed index to evaluate voltage stability in radial distribution systems over a 24-hour period. This approach would allow the assessment of the index's capability to monitor vulnerable areas (critical buses and lines) and prevent voltage collapse under varying load conditions and uncertainties associated with renewable energy sources (RESs). While such approaches have been explored for transmission systems, such as in [45], using the critical eigenvalue index, their application in distribution systems remains largely unexplored.
- Continued progress in vehicle-to-grid (V2G) technology offers significant potential to enhance grid stability and optimize energy management. A study [46] proposed an optimized charging and discharging strategy based on a stability index. This ap-

proach can be further improved by incorporating the proposed *NDVSI* as an objective function within advanced optimization frameworks to reduce the risk of instability. As large-scale electric vehicle (EV) charging across multiple load buses can exacerbate voltage collapse, the *NDVSI* provides a meaningful stability signal. Its value remains close to unity under stable operating conditions and decreases toward zero as the system approaches voltage collapse. Therefore, maximizing the *NDVSI*, as formulated in Equation (14), enables the determination of optimal EV charging and discharging power ratings for maintaining voltage stability throughout both daytime and nighttime periods.

$$\max\left(\sum_{t=1}^{24}\sum_{1}^{Bus\ No.} V_i^2 \sin^2(\theta-\delta+45^\circ) - 2\sqrt{2}Z(P_j+Q_j)\sin(\theta+45^\circ)\right) \quad (14)$$

In this way, the profile of the voltage stability index can be determined during the day and at night to assess the stability. In addition, the load profile can be determined. *NDVSI* can be tested as objective functions to check the improvement in voltage stability and determine the allowable loads of EVs.

Author Contributions: Conceptualization, S.M., Y.W., M.A. and M.A.I.; methodology, S.M.; software, S.M.; validation, S.M.; formal analysis, S.M.; investigation, S.M.; resources, S.M.; data curation, S.M.; writing—original draft preparation, S.M.; writing—review and editing, S.M., Y.W., M.A. and M.A.I.; visualization, S.M.; supervision, Y.W., M.A. and M.A.I.; project administration, Y.W., M.A. and M.A.I.; funding acquisition, M.A. All authors have read and agreed to the published version of the manuscript.

Funding: This research was funded by the Deanship of Scientific Research at Northern Border University, Arar, KSA (project number NBU-FFR-2025-2124-02).

Data Availability Statement: The data for the three industrial systems, namely the IEEE 12-bus, IEEE 33-bus and IEEE 69-bus systems, can be found in references [47–49].

Acknowledgments: The authors extend their appreciation to the Deanship of Scientific Research at Northern Border University, Arar, KSA, for funding this research (project number NBU-FFR-2025-2124-02).

Conflicts of Interest: The authors declare no conflicts of interest.

Abbreviations

The abbreviations listed below are used throughout this manuscript:

SI	Stability index
NDVSI	Novel distribution voltage stability index
CB	Critical bus
CL	Critical line
PSI	Power stability index
BFOA	Foraging optimization algorithm
HPSO	Hybrid practical swarm optimization
BSOA	Backtracking search optimization algorithm
SKHA	Stud krill herd algorithm
MOWOA	Multi-objective whale optimization algorithm
CSA	Crow search algorithm
OTCDE	Opposition-based tuned-chaotic differential evolution
BIBC	Bus injection to branch current
VSI	Voltage sensitivity index
DFA	Dragonfly algorithm
IPSO	Improved particle swarm optimization
N. A	Not analyzed

APSFS	Active power supplied from the substation
RPSFS	Reactive power supplied from the substation
AELC	Annual energy loss cost
ELCS	The energy loss cost saving
RRCEL	The reduction rate in the cost of energy losses

Nomenclature

The parameters applied in this study are presented below to assist the reader.

Z	The impedance of the distribution line
R	The resistance of the distribution line
X	The reactance of the distribution line
θ	The impedance angle
Y	The shunt admittance of line

The definitions of variables and terms used throughout this work are outlined as follows.

I_i	The branch current at the sending bus
I_j	The branch current at the receiving bus
V_i	The voltage at the sending bus
V_j	The voltage at the receiving bus
δ_i	The voltage angle at the sending bus
δ_j	The voltage angle at the receiving bus
S_i	The apparent power at the sending bus
S_j	The apparent power at the receiving bus
pf	Power factor
λ	The total load at the base loading case
$\lambda_{\max}$	The maximum loading (critical load)
P_{loss}	The active power loss
Q_{loss}	The reactive power loss
E_c	The energy cost
T_d	The time duration
$C(P_{dg})$	The cost of generated active power of distributed generator
$C(Q_{dg})$	The cost of generated reactive power of distributed generator
$S_{g\max}$	The maximum generated complex power from the distributed generator

References

1. Yammani, C.; Maheswarapu, S.; Matam, S.K. A Multi-objective Shuffled Bat algorithm for optimal placement and sizing of multi distributed generations with different load models. *Int. J. Electr. Power Energy Syst.* **2016**, *79*, 120–131. [CrossRef]
2. Mokred, S.; Wang, Y.; Chen, T. A novel collapse prediction index for voltage stability analysis and contingency ranking in power systems. *Prot. Control Mod. Power Syst.* **2023**, *8*, 1–27. [CrossRef]
3. Christa, S.A.S.T.J.; Suresh, S. Enhancing grid resilience and efficiency with distributed generators through fuzzified firefly optimization. *Electr. Eng.* **2024**, *106*, 7803–7818. [CrossRef]
4. Kalarathi, S.A.M.; Bhuvanesh, S.S.A. Multi-objective optimal distributed generators integration using firefly algorithm with Fuzzy decision making. *Electr. Eng.* **2024**, *106*, 6113–6130. [CrossRef]
5. W. G. CIGRE and Working Group 37.23, "Impact of Increasing Contribution of Dispersed Generation on the Power System-Final Report," Electra, Sept., no. February, 1998, [Online]. Available online: https://books.google.com/books?id=hGIvMwAACAAJ (accessed on 15 January 2025).
6. Mostafa, M.H.; Elshahed, M.A.; Elmarsfawy, M.M. Power Flow Study and Voltage Stability Analysis for Radial System with Distributed Generation. *Int. J. Comput. Appl.* **2016**, *137*, 19–26. [CrossRef]
7. Malik, S.; Modi, B.; Mangrolia, D. Grid Integration of Distributed Generation: Issues and Challenges. In Proceedings of the 2022 International Conference for Advancement in Technology (ICONAT), Goa, India, 21–22 January 2022; pp. 1–6. [CrossRef]
8. Ehsan, A.; Yang, Q. Optimal integration and planning of renewable distributed generation in the power distribution networks: A review of analytical techniques. *Appl. Energy* **2018**, *210*, 44–59. [CrossRef]
9. Reddy, P.D.P.; Reddy, V.C.V.; Manohar, T.G. Application of flower pollination algorithm for optimal placement and sizing of distributed generation in Distribution systems. *J. Electr. Syst. Inf. Technol.* **2016**, *3*, 14–22. [CrossRef]
10. Avar, A.; Sheikh-El-Eslami, M.K. Optimal DG placement in power markets from DG Owners' perspective considering the impact of transmission costs. *Electr. Power Syst. Res.* **2021**, *196*, 107218. [CrossRef]

11. Türkoğlu, A.S.; Güldorum, H.C.; Sengor, I.; Çiçek, A.; Erdinç, O.; Hayes, B.P. Maximizing EV profit and grid stability through Virtual Power Plant Considering V2G. *Energy Rep.* **2024**, *11*, 3509–3520. [CrossRef]
12. Werkie, Y.G.; Kefale, H.A. Optimal allocation of multiple distributed generation units in power distribution networks for voltage profile improvement and power losses minimization. *Cogent Eng.* **2022**, *9*, 1–23 2091668. [CrossRef]
13. Devabalaji, K.R.; Ravi, K. Optimal size and siting of multiple DG and DSTATCOM in radial distribution system using Bacterial Foraging Optimization Algorithm. *Ain Shams Eng. J.* **2016**, *7*, 959–971. [CrossRef]
14. Suresh, M.C.V.; Belwin, E.J. Optimal DG placement for benefit maximization in distribution networks by using Dragonfly algorithm. *Renew. Wind Water Sol.* **2018**, *5*, 4. [CrossRef]
15. El-Fergany, A. Optimal allocation of multi-type distributed generators using backtracking search optimization algorithm. *Int. J. Electr. Power Energy Syst.* **2015**, *64*, 1197–1205. [CrossRef]
16. Ali, E.S.; Abd Elazim, S.M.; Abdelaziz, A.Y. Ant Lion Optimization Algorithm for optimal location and sizing of renewable distributed generations. *Renew. Energy* **2017**, *101*, 1311–1324. [CrossRef]
17. Wang, Z.; Chen, B.; Wang, J.; Kim, J.; Begovic, M.M. Robust optimization based optimal DG placement in microgrids. *IEEE Trans. Smart Grid* **2014**, *5*, 2173–2182. [CrossRef]
18. Aman, M.M.; Jasmon, G.B.; Bakar, A.H.A.; Mokhlis, H. A new approach for optimum simultaneous multi-DG distributed generation Units placement and sizing based on maximization of system loadability using HPSO (hybrid particle swarm optimization) algorithm. *Energy* **2014**, *66*, 202–215. [CrossRef]
19. ChithraDevi, S.A.; Lakshminarasimman, L.; Balamurugan, R. Stud Krill herd Algorithm for multiple DG placement and sizing in a radial distribution system. *Eng. Sci. Technol. Int. J.* **2017**, *20*, 748–759. [CrossRef]
20. Hari Prasad, C.; Subbaramaiah, K.; Sujatha, P. Optimal DG unit placement in distribution networks by multi-objective whale optimization algorithm & its techno-economic analysis. *Electr. Power Syst. Res.* **2023**, *214*, 108869. [CrossRef]
21. Ismael, S.M.; Aleem, S.H.E.A.; Abdelaziz, A.Y. Optimal sizing and placement of distributed generation in Egyptian radial distribution systems using crow search algorithm. In Proceedings of the 2018 International Conference on Innovative Trends in Computer Engineering (ITCE), Aswan, Egypt, 19–21 February 2018; pp. 332–337. [CrossRef]
22. Manna, D.; Goswami, S.K. Optimum placement of distributed generation considering economics as well as operational issues. *Int. Trans. Electr. Energy Syst.* **2020**, *30*, 1–20. [CrossRef]
23. Kumar, S.; Mandal, K.K.; Chakraborty, N. A novel opposition-based tuned-chaotic differential evolution technique for techno-economic analysis by optimal placement of distributed generation. *Eng. Optim.* **2020**, *52*, 303–324. [CrossRef]
24. Acharya, N.; Mahat, P.; Mithulananthan, N. An analytical approach for DG allocation in primary distribution network. *Int. J. Electr. Power Energy Syst.* **2006**, *28*, 669–678. [CrossRef]
25. Hung, D.Q.; Mithulananthan, N. Multiple distributed generator placement in primary distribution networks for loss reduction. *IEEE Trans. Ind. Electron.* **2013**, *60*, 1700–1708. [CrossRef]
26. Murty, V.V.S.N.; Kumar, A. Optimal placement of DG in radial distribution systems based on new voltage stability index under load growth. *Int. J. Electr. Power Energy Syst.* **2015**, *69*, 246–256. [CrossRef]
27. Elsaiah, S.; Benidris, M.; Mitra, J. Analytical approach for placement and sizing of distributed generation on distribution systems. *IET Gener. Transm. Distrib.* **2014**, *8*, 1039–1049. [CrossRef]
28. Ettehadi, M.; Ghasemi, H.; Vaez-Zadeh, S. Voltage stability-based DG placement in distribution networks. *IEEE Trans. Power Deliv.* **2013**, *28*, 171–178. [CrossRef]
29. Hung, D.Q.; Mithulananthan, N.; Lee, K.Y. Optimal placement of dispatchable and nondispatchable renewable DG units in distribution networks for minimizing energy loss. *Int. J. Electr. Power Energy Syst.* **2014**, *55*, 179–186. [CrossRef]
30. Murthy, V.V.S.N.; Kumar, A. Comparison of optimal DG allocation methods in radial distribution systems based on sensitivity approaches. *Int. J. Electr. Power Energy Syst.* **2013**, *53*, 450–467. [CrossRef]
31. Wang, C.; Nehrir, M.H. Analytical approaches for optimal placement of distributed generation sources in power systems. *IEEE Trans. Power Syst.* **2004**, *19*, 2068–2076. [CrossRef]
32. Aman, M.M.; Jasmon, G.B.; Mokhlis, H.; Bakar, A.H.A. Optimal placement and sizing of a DG based on a new power stability index and line losses. *Int. J. Electr. Power Energy Syst.* **2012**, *43*, 1296–1304. [CrossRef]
33. Alrashidi, M.R.; Alhajri, M.F. Optimal planning of multiple distributed generation sources in distribution networks: A new approach. *Energy Convers. Manag.* **2011**, *52*, 3301–3308. [CrossRef]
34. Mokred, S.; Lijun, Q.; Kamara, G. Smart Design of Distribution Series Capacitor Bank Application for Improved Voltage Quality and Motor Start. In Proceedings of the 2020 IEEE/IAS Industrial and Commercial Power System Asia (I&CPS Asia), Weihai, China, 13–15 July 2020; pp. 454–459. [CrossRef]
35. Mokred, S.; Lijun, Q.; Khan, T. Protection Performance during Application of an Intelligent and Fast Switch Series Capacitor to 25kV Radial Power Distribution Network. In Proceedings of the 2020 IEEE/IAS Industrial and Commercial Power System Asia (I&CPS Asia), Weihai, China, 13–15 July 2020; pp. 921–928. [CrossRef]

36. Mokred, S.; Lijun, Q.; Kamara, G.; Khan, T. Comparison of the Effect of Series and Shunt Capacitor Application in 25kV Radial Power Distribution Network. In Proceedings of the 2020 IEEE/IAS Industrial and Commercial Power System Asia (I&CPS Asia), Weihai, China, 13–15 July 2020; pp. 822–830. [CrossRef]
37. Chakravorty, M.; Das, D. Voltage stability analysis of radial distribution networks. *Electr. Power Energy Syst.* **2001**, *23*, 129–135. [CrossRef]
38. Ranjan, R.; Venkatesh, B.; Das, D. Voltage stability analysis of radial distribution networks. *Electr. Power Compon. Syst.* **2003**, *31*, 501–511. [CrossRef]
39. Eminoglu, U.; Hocaoglu, M.H. A Voltage stability index for radial distribution networks. In Proceedings of the 42nd International Universities Power Engineering Conference, Brighton, UK, 4–6 September 2007; pp. 408–413. [CrossRef]
40. Abul'Wafa, A.R. A network-topology-based load flow for radial distribution networks with composite and exponential load. *Electr. Power Syst. Res.* **2012**, *91*, 37–43. [CrossRef]
41. Gautam, D.; Mithulananthan, N. Optimal DG placement in deregulated electricity market. *Electr. Power Syst. Res.* **2007**, *77*, 1627–1636. [CrossRef]
42. Gözel, T.; Eminoglu, U.; Hocaoglu, M.H. A tool for voltage stability and optimization (VS&OP) in radial distribution systems using matlab graphical user interface (GUI). *Simul. Model. Pract. Theory* **2008**, *16*, 505–518. [CrossRef]
43. Muthukumar, K.; Jayalalitha, S. Optimal placement and sizing of distributed generators and shunt capacitors for power loss minimization in radial distribution networks using hybrid heuristic search optimization technique. *Int. J. Electr. Power Energy Syst.* **2016**, *78*, 299–319. [CrossRef]
44. Kansal, S.; Kumar, V.; Tyagi, B. Hybrid approach for optimal placement of multiple DGs of multiple types in distribution networks. *Int. J. Electr. Power Energy Syst.* **2016**, *75*, 226–235. [CrossRef]
45. Rahman, S.; Saha, S.; Haque, M.E.; Islam, S.N.; Arif, M.T.; Mosadeghy, M.; Oo, A.M.T. A framework to assess voltage stability of power grids with high penetration of solar PV systems. *Int. J. Electr. Power Energy Syst.* **2022**, *139*, 107815. [CrossRef]
46. Kim, H.Y.; Shin, G.S.; Mahseredjian, J.; Kim, C.H. Voltage Stability Index (VSI)-Based Optimal Vehicle-to-Grid(V2G) Charging/Discharging Strategy in Radial Distribution System. *J. Electr. Eng. Technol.* **2024**, *19*, 3885–3890. [CrossRef]
47. Das, D.; Nagi, H.S.; Kothari, D.P. Novel method for solving radial distribution networks. *IEE Proc. Gener. Transm. Distrib.* **1994**, *141*, 291–298. [CrossRef]
48. Vita, V. Development of a decision-making algorithm for the optimum size and placement of distributed generation units in distribution networks. *Energies* **2017**, *10*, 1433. [CrossRef]
49. Abdul kadir, A.F.; Mohamed, A.; Shareef, H.; Che Wanik, M.Z. Optimal placement and sizing of distributed generations in distribution systems for minimizing losses and THDv using evolutionary programming. *Turk. J. Electr. Eng. Comput. Sci.* **2013**, *21*, 2269–2282. [CrossRef]

Disclaimer/Publisher's Note: The statements, opinions and data contained in all publications are solely those of the individual author(s) and contributor(s) and not of MDPI and/or the editor(s). MDPI and/or the editor(s) disclaim responsibility for any injury to people or property resulting from any ideas, methods, instructions or products referred to in the content.